Classification of ADHD by Using Multiple Feature Maps of EEG Signals and Deep Feature Extraction

Ozlem Karabiber Cura
Dept. of Biomedical Eng.
Izmir Katip Celebi University
Izmir, TURKEY
ozlem.karabiber@ikcu.edu.tr

Sibel Kocaaslan Atli
Dept. of Biophysics
Izmir Katip Celebi University
Izmir, TURKEY
sibel.atli@ikcu.edu.tr

Sena Yagmur Sen and Aydin Akan
Dept. of Electrical and Electronics Eng.
Izmir University of Economics
Izmir, TURKEY
akan.aydin@ieu.edu.tr

***Abstract*—Attention Deficit Hyperactivity Disorder (ADHD) is a neurological condition, typically manifesting in childhood. Behavioral studies are used to treat the illness, but there is no conclusive way to diagnose it. In order to comprehend changes in the brain, electroencephalography (EEG) signals of ADHD patients are frequently examined. In the proposed study, we introduced EEG feature maps (EEG-FM)-based image construction to be used as input to CNN architectures. To demonstrate the effectiveness of the proposed method, EEG data of 15 ADHD patients and 18 control subjects are analyzed and ADHD detection performance is demonstrated. EEG-FM-based images are obtained using both time domain features such as Hjorth parameters (activity, mobility, complexity), skewness, kurtosis, and peak-to-peak, and nonlinear features such as largest Lyapunov Exponent, correlation dimension, Hurst exponent, Katz fractal dimension, Higuchi fractal dimension, and approximation entropy. ResNet18 is trained using EEG-FM-based images and deep features are extracted for each image subset. Using the SVM classifier, the ADHD detection performance of the proposed approach is evaluated. Experimental results revealed that using EEG-FM-based images as input to ResNet architecture offers important benefits in identifying ADHD.**

***Index Terms*—Attention Deficit Hyperactivity Disorder (ADHD), EEG Feature maps, deep feature extraction, machine learning.**

I. Introduction

Children and teenagers are frequently affected by the behavioral neurodevelopmental disease named Attention-Deficit/Hyperactivity Disorder (ADHD), which has the potential to have long-term effects [1], [2]. The prevalence of this condition is estimated to be 2.5% in adults and 5% in children. ADHD may also coexist with mental illnesses like depression or bipolar disorder and is defined by a predominance of inattention, hyperactivity, and impulsivity alone or in combination [1]–[3]. ADHD is frequently identified using data from the patient, their teachers, and their parents, and questionnaires. The doctor's training has an effect on this arbitrary diagnosis. Hence, the diagnosis of ADHD may be challenging, and mistakes are frequently made [1], [2].

EEG analysis under different cognitive tasks or in the resting state is of great interest to researchers for the detection of ADHD due to the easy accessibility, inexpensiveness, and non-invasiveness of EEG [3], [4]. The total power, absolute power, and relative power of several EEG frequency bands, such as delta ($\leq$ 4 Hz), theta (4–8 Hz), alpha (8–13 Hz), beta (13–30 Hz), and gamma ($\geq$ 30 Hz), have all been examined in numerous studies to detect ADHD [3]–[6]. The numerous complexity-based non-linear features such as entropy (approximate, sample, permutation, and wavelet entropy), Higuchi fractal dimension, Katz fractal dimension, Hurst exponent, Lempel-Ziv complexity, largest Lyapunov exponent, and correlation dimension have also been computed as features in many studies [3], [4], [7]–[11]. The differences and similarities between intra-hemispheric or inter-hemispheric EEG channel pairs have been also examined by using a variety of analysis methods and features such as magnitude square coherence [4], [12], bispectral analysis [5], dynamic frequency warping (DFW) [1], synchronization likelihood (SL) [13].

This paper presents the CNN and novel EEG Feature map-based ADHD classification technique. This is accomplished by creating new EEG Feature Maps-based input data for training the model, followed by the use of ResNet18-based deep learning architecture for feature extraction and a variety of machine learning algorithms for classification.

II. Material and Method

The placements of the EEG electrodes or the EEG topography for a particular EEG segment are often not taken into account when applying the EEG features. This work aims to demonstrate the benefits of CNN-based feature extraction models and EEG feature maps for representing the spatial and spectral information of individual EEG segments. In order to detect ADHD EEG segments, a sophisticated CNN-based model is created by computing the numerous linear and non-linear EEG properties. Our hybrid model uses a CNN for deep feature extraction and machine learning approaches for classification to categorize the EEG segments of ADHD patients and control subjects.

A. ADHD EEG dataset

The Brain Vision system at the Izmir Katip Celebi University is used to capture EEG data from 15 ADHD patients (7 boys, 8 girls, average age: 12) and 18 control subjects (CS) (4 boys, 14 girls, average age: 13). The used EEG signals are recorded from 30 different channels (Fp1, Fp2, F7, F8, F3, F4, Fz, FT7, FT8, FC3, FC4, FCz, T3, T4, C3, C4, Cz, TP7, TP8, CP3, CP4, CPz, T5, T6, P3, P4, Pz, O1, O2, Oz) at a sampling

frequency of 1 kHz using an internationally established 10-20 electrode placement technique. Each participant's EEG signal was recorded for a total of 4 minutes while they were in the open-eyes resting state. Ethical approval dated 11.07.2019 and numbered 76 is acquired from the non-interventional clinical research ethics committee of the Izmir Katip Celebi University for the collection of EEG data utilized in this work. Each channel is filtered with a Butterworth band-pass filter with a $[0.5 - 50]$ Hz cutoff frequency to lessen power line interference and other disturbances. Each channel's EEG data is also separated into segments with a 5-second length.

B. EEG features Calculation and Topo-FM Construction

It is crucial to choose the features that will be used to compute the features in order to expose unique information about the signal. The EEG signals may be used to extract several linear and nonlinear features for both the time domain and frequency domain or the time-frequency domain, as was also indicated in the introduction section. In our study, to extract the time domain and nonlinear features, the raw EEG signals with a 5 s duration are employed. To generate EEG Topo FMs, we simply employed six time-domain features and six non-linear features, despite the fact that more complex features are frequently used by researchers. The time domain features: Hjorth activity (HA), mobility (HM) and complexity (HC), peak-to-peak (PTP), skewness (SKW), and kurtosis (KTS) [14], [15], and the non-linear features: Largest Lyapunov Exponent (LLE) [7]–[11], Correlation Dimension (CD) [9], [10], Fractal Dimensions (Higuchi (HFD) and Katz's (KFD)) [7]–[9], Hurst Exponent (HE) [8], and Approximate Entropy (ApEn) [4], [7], [9], [11] are selected for our study. Calculated feature values are then normalized using max-min normalization methods for obtained time domain and nonlinear feature sets.

The EEG Topo-FM is generated as the last step. The normalized feature values of a subject's 30 EEG channels are positioned using the 10-20 electrode placements technique (shown in Fig 1-up). According to the dataset, electrode placements are mapped on the, 9×9 feature matrix as shown in Fig 1-middle [14], [16]. The normalized feature values are instantly inserted into the red spots in the feature matrix. The values of the gray points are calculated as a function of the point values around them as mentioned in the study [16] using the following formulation;

$$K_{(i,j)} = \frac{K'_{(i+1,j)} + K'_{(i-1,j)} + K'_{(i,j+1)} + K'_{(i,j-1)}}{M}, \quad (1)$$

where $0 \leq i, j \leq 8$, K denotes the normalized feature value of the gray point, K' indicates the normalized value of the point neighboring this point. The number of non-zero components in the numerator is indicated by the default value of M, which is 1.

Then, by interpolating the matrix's empty spaces and employing a "jet" colormap, a fully EEG Topo-FM of a specific feature is created. MATLAB 2022b is used throughout the whole process of creating EEG-FMs, and the results are saved as.png images with a 224×224 pixel resolution.

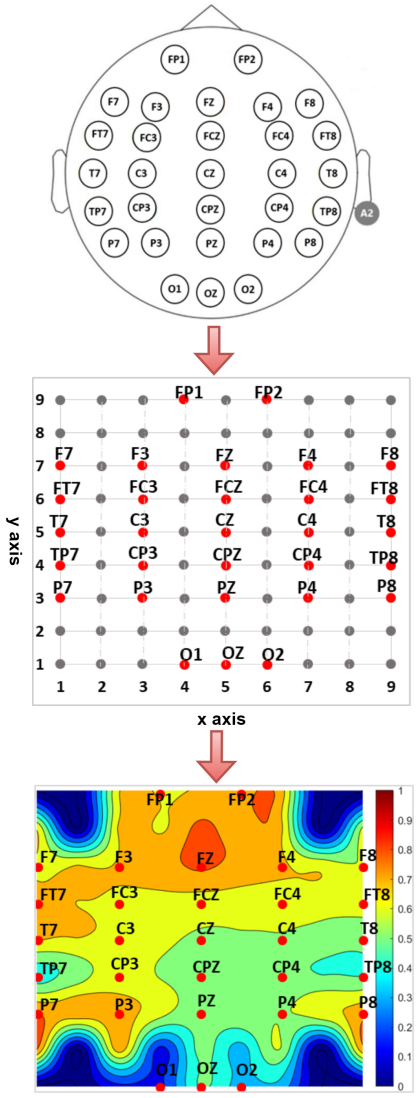

Fig. 1: ADHD patient 10-20 electrode mapping on the 9x9 matrix and EEG Topo-FM example.

As an example, Fig.1-down provides the EEG Topo-FM of one ADHD patient's first EEG segment that was derived utilizing the skewness feature. In terms of the "jet" colormap, the red color identifies active electrodes whereas the dark blue color denotes a fully inactive electrode. Each electrode's coordinates are established in accordance with the 10–20 electrode mapping on the 9×9 matrix presented in Fig 1-middle. For instance, the coordinate of the frontal electrode Fp2 is (6,9) and those of the temporal electrode T8 is (9,5). The frontal region in the ADHD patient has shown significant activation in this EEG segment, which is noted in Fig.1-down.

C. ResNet18 based Feature Extraction

The initial stage in our suggested methodology is to create EEG-FMs (224×224 sizes) derived utilizing various EEG

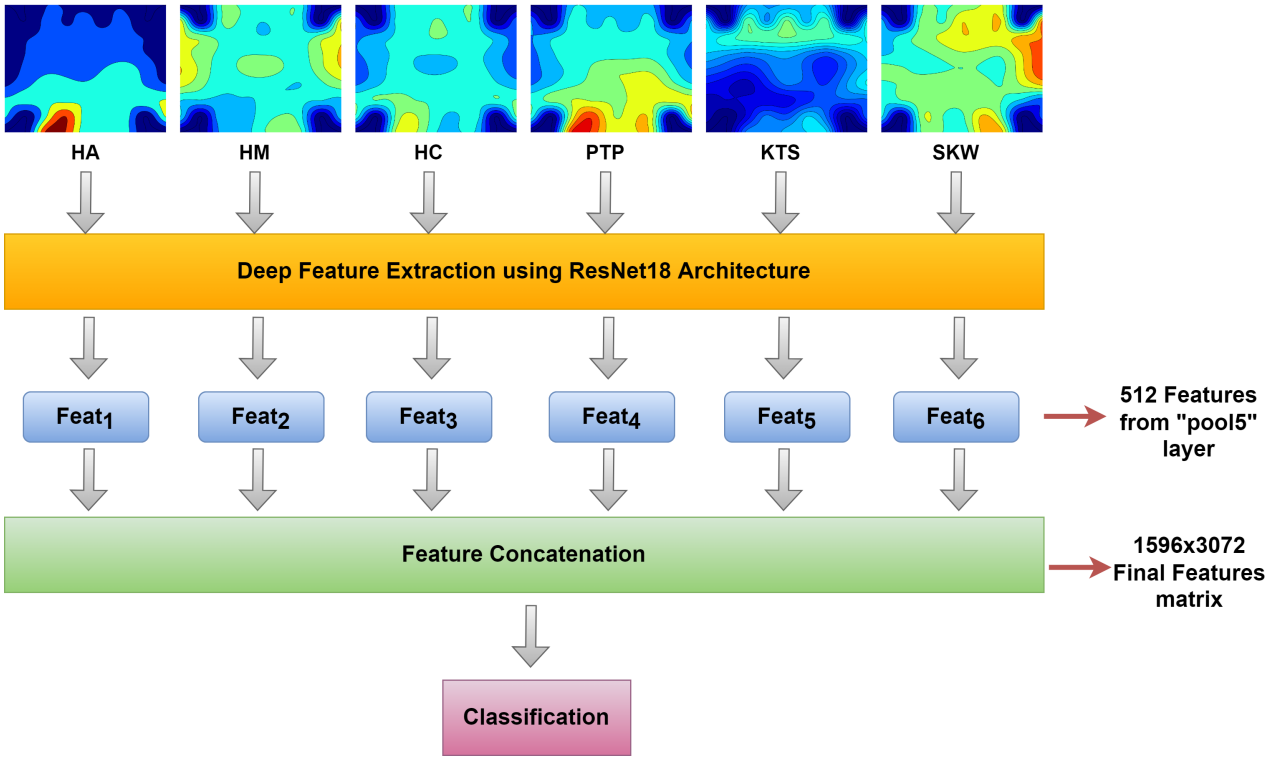

Fig. 2: Flowchart illustrating the procedures for extracting, fusing, and classifying deep features.

features. EEG-FM-based image data sets are created using both time-domain (HA, HM, and HC, PTP, SKW, and KTS) [14], [15] and nonlinear (ApEn, CD, HE, HFD, KFD, and LLE) [8]–[10] EEG features. Therefore, six independent image subsets are created for both the time domain and nonlinear features, and these two distinct feature domains are taken into account separately for our analysis. The ResNet-18 architecture is then utilized for feature extraction using a transfer learning approach. Because this architecture trains images quicker than others without losing performance. With each layer that is added, convolutional neural networks go deeper and deeper, but as soon as the accuracy reaches saturation, it swiftly declines. ResNets, which are based on residuals or skip connections, was created to address this problem. Identity and convolutional blocks make up the majority of ResNets. There are several ResNet versions, including ResNet-18, ResNet-50, ResNet-101, and ResNet-152. ResNet18 which has 11 million parameters and 18 layers, is utilized for our study [17].

Each EEG-FM-based image subset of the time domain and nonlinear features is utilized to extract 512 deep features using the "pool5" layer of ResNet18. For instance, we have six separate EEG-FM-based image subsets for the time domain: ApEn, HA, HM, HC, SKW, and KTS. After obtaining 512 features for each of these image subsets, the feature fusion method is carried out. The process is presented using equations 2 and 3. The same techniques are used for nonlinear EEG-FM-based image subsets.

$$F^i = Res18(I^i); \qquad i \in \{1, 2, 3, 4, 5, 6\} \tag{2}$$

Here I^i is the i^{th} image subsets of feature space and the feature generator for ResNet18 is defined by Res18(.). F^i indicates the created i^{th} deep feature vector with a length of 512.

$$F_{con}(j + 512 \times (k-1)) = F^k(j);\ j \in \{1, 2, ..., 512\},\ k \in \{1, 2, ..., 6\} \tag{3}$$

Here F_{con} is concatenated features with a length of 3072. 512 features are extracted from each EEG-FM-based image subset in this stage of the model (6 image subsets for each feature space). $6 \times 512 = 3072$ features are derived in this manner from image subsets. Fig. 2 shows the proposed feature extraction, fusion, and classification procedure of ResNet18.

D. Classification and performance Evaluations

The model's classification performance is evaluated using several machine learning algorithms, including decision tree (DT) [8], k-nearest neighbor (kNN) [3], [8], [10], support vector machine (SVM) [3], [8], [9], [11], and Random Forest (RF) [8]. To verify the model, a 10-fold cross-validation technique is utilized with a medium Gaussian SVM. Performance is assessed using a variety of statistical measures, including accuracy (ACC), sensitivity (SEN), selectivity (SPE), positive predictive values (PPV), and false discovery rate (FDR) [2], [15].

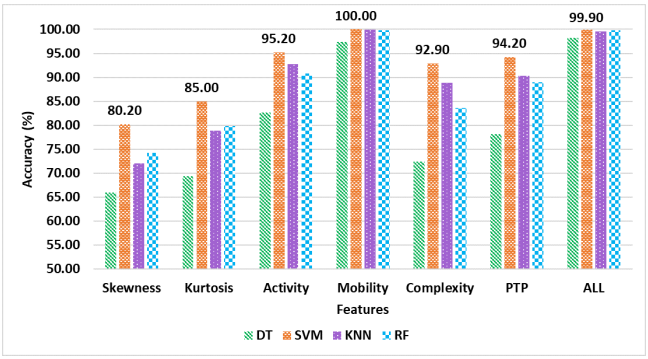

(a)

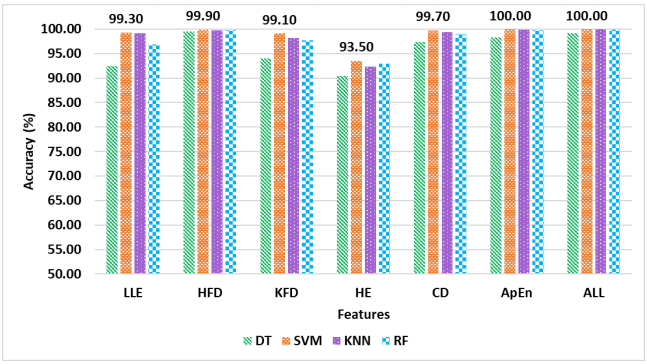

(b)

Fig. 3: Performance accuracy of proposed EEG feature map-based CNN model for (a) time domain features, and (b) Nonlinear features.

III. RESULTS AND DISCUSSION

In this study, ADHD and control EEG data are used to investigate the performance of the proposed EEG-FM-based images using Resnet18 architecture for the classification. The EEG-FM-based image subsets generated using both time domain and nonlinear features are considered as input to the Resnet-18 and deep features are extracted for each of them. Then, the classification process is conducted for both feature spaces separately.

TABLE I: Overall two-class classification performance of proposed approach for time domain (TimeF) and nonlinear (NonLF) features obtained using SVM classifier.

Feature Space	Feature	ACC	SEN	SPE	PPV	FDR
TimeF	**SKW**	80.2	71.8	86.40	79.8	20.2
	KTS	85.0	76.2	91.5	86.9	13.1
	HA	95.2	92.1	97.5	96.5	3.5
	HM	100.0	100.0	100.0	100.0	0.0
	HC	92.9	90.0	95.0	93.0	7.0
	PTP	94.2	91.9	95.8	94.3	5.7
	ALL	99.9	100.0	99.8	99.7	0.3
NonLF	**LLE**	99.3	98.6	99.9	99.9	0.1
	HFD	99.9	99.7	100.0	100.0	0.0
	KFD	99.1	98.2	99.9	99.9	0.1
	HE	93.5	93.0	93.9	92.8	7.2
	CD	99.7	99.5	99.9	99.9	0.1
	ApEn	100.0	100.0	100.0	100.0	0.0
	ALL	100.0	100.0	100.0	100.0	0.0

Performance accuracies of the proposed method for different individual EEG-FM-based image subsets are presented in Fig.3. It is noticed that the proposed approach yields high classification accuracies for both individual image subsets and concatenated feature sets ("ALL"). Moreover, higher classification accuracies are obtained using the SVM classifier for both feature spaces and each case (TimeF: $\geq$ 80.20, NonLF: $\geq$ 93.50). Therefore, detailed analyses are conducted using the SVM classifier and different performance evaluation metrics. Table I summarizes the classification results of the proposed approach in terms of SEN, SPE, PPV, FDR, and ACC for the SVM classifier. The classification accuracy of deep features obtained using EEG-FM-based inputs for time domain features is higher than 80.2%. On the other hand, deep features obtained utilizing EEG-FM-based images provide classification accuracies for the nonlinear features that are higher than 93.5 %. For both feature spaces, concatenated feature sets yield higher classification performances (TimeF: 99.9% ACC, 100.0 % SEN, 99.8% SPE, 99.7% PPV, and 0.3% FDR; NonLF: 100.0% ACC, 100.0 % SEN, 100.0 % SPE, 100.0 % PPV, and 0.0% FDR).

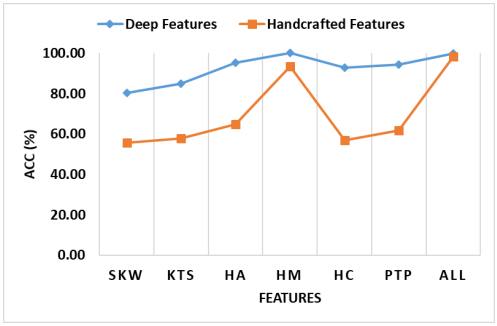

(a)

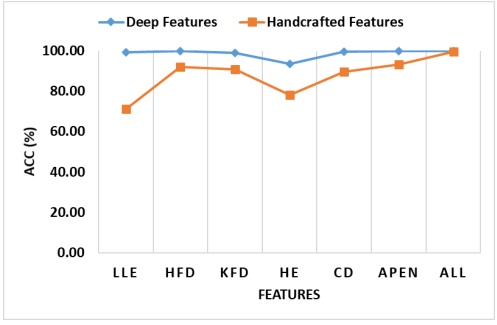

(b)

Fig. 4: Utilizing the SVM classifier, comparison of the classification performances of deep features obtained using the ResNet18 architecture in which EEG-FM-based images are used as input, and that of handcrafted features; for (a) time domain features, and (b) Nonlinear features.

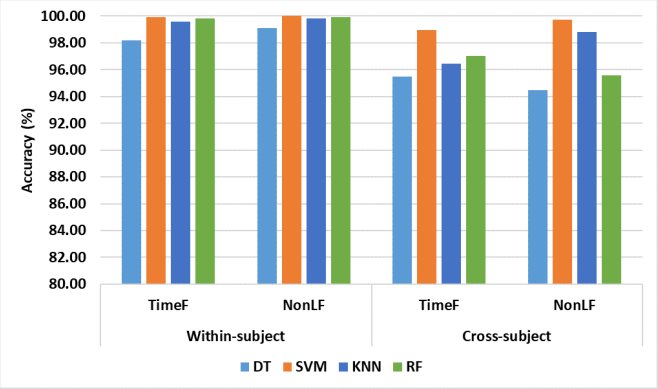

Fig. 5: Performance comparison of within-subject and cross-subject paradigm for EEG-FM based deep features.

In order to demonstrate the advantages of the proposed method, a performance comparison of deep features obtained using the ResNet18 architecture from the EEG-FM-based images, and 1D handcrafted features is conducted. In this comparison, the SVM classifier is utilized and classification performances are obtained in terms of ACC for six different time domains and nonlinear features (given in Figure 4). Considering both individual features and their combinations, EEG-FM-based inputs provide higher accuracies for each feature domain. Especially for time domain features, the classification accuracy of handcrafted features dropped below 60%. The combination of both deep features and handcrafted features provides nearly equal classification accuracies. However, for the individual features, deep features outperformed. This shows that the created feature maps contain quality information because they contain both temporal and spatial information.

In order to complicate the problem and reveal the effectiveness of the proposed EEG-FM-based deep feature model more clearly, the classification accuracies are also measured using within-subject and cross-subject paradigms. The within-subject paradigm used a portion of the data for each subject to train the model and the remainder to test. During the cross-subject paradigm, data from other participants is utilized to train the model, while data from a subject that is not used to train the model is used for testing. The performance comparison is given in Figure 5. We found that in the within-subject paradigm, all four classifiers satisfy nearly perfect accuracy $\geq 98\%$, and in the cross-subject paradigm, all four classifiers provide higher accuracy $\geq 94\%$.

IV. Conclusion

In this study, we introduce a new image representation of the features extracted from two classes of ADHD-EEG signals. These feature map-based images may be used as input to CNN architectures for biomedical applications. The advantages of the proposed approach are demonstrated in the classification problem of ADHD and control subjects' EEG segments. The experimental results of the proposed study show that the use of EEG-FM-based images as input to the ResNet architecture provides significant improvement in the detection of ADHD. In our future study, we consider the application of various feature selection methods before the feature concatenation step to further improve classification performance.

References

[1] P. Ghaderyan, F. Moghaddam, S. Khoshnoud, and M. Shamsi, "New interdependence feature of EEG signals as a biomarker of timing deficits evaluated in attention-deficit/hyperactivity disorder detection," *Measurement*, vol. 199, p. 111468, 2022.

[2] M. Bakhtyari and S. Mirzaei, "Adhd detection using dynamic connectivity patterns of EEG data and ConvLSTM with attention framework," *Biomedical Signal Processing and Control*, vol. 76, p. 103708, 2022.

[3] M. Altınkaynak, N. Dolu, A. Güven, F. Pektaş, S. Özmen, E. Demirci, and M. İzzetoğlu, "Diagnosis of attention deficit hyperactivity disorder with combined time and frequency features," *Biocybernetics and Biomedical Engineering*, vol. 40, no. 3, pp. 927–937, 2020.

[4] J. J. González, L. D. Méndez, S. Mañas, M. R. Duque, E. Pereda, and L. De Vera, "Performance analysis of univariate and multivariate EEG measurements in the diagnosis of adhd," *Clinical Neurophysiology*, vol. 124, no. 6, pp. 1139–1150, 2013.

[5] H. Chen, W. Chen, Y. Song, L. Sun, and X. Li, "EEG characteristics of children with attention-deficit/hyperactivity disorder," *Neuroscience*, vol. 406, pp. 444–456, 2019.

[6] A. Tenev, S. Markovska-Simoska, L. Kocarev, J. Pop-Jordanov, A. Müller, and G. Candrian, "Machine learning approach for classification of adhd adults," *International Journal of Psychophysiology*, vol. 93, no. 1, pp. 162–166, 2014.

[7] M. R. Mohammadi, A. Khaleghi, A. M. Nasrabadi, S. Rafieivand, M. Begol, and H. Zarafshan, "EEG classification of adhd and normal children using non-linear features and neural network," *Biomedical Engineering Letters*, vol. 6, no. 2, pp. 66–73, 2016.

[8] H. T. Tor, C. P. Ooi, N. S. Lim-Ashworth, J. K. E. Wei, V. Jahmunah, S. L. Oh, U. R. Acharya, and D. S. S. Fung, "Automated detection of conduct disorder and attention deficit hyperactivity disorder using decomposition and nonlinear techniques with EEG signals," *Computer Methods and Programs in Biomedicine*, vol. 200, p. 105941, 2021.

[9] Y. K. Boroujeni, A. A. Rastegari, and H. Khodadadi, "Diagnosis of attention deficit hyperactivity disorder using non-linear analysis of the EEG signal," *IET systems biology*, vol. 13, no. 5, pp. 260–266, 2019.

[10] F. Ghassemi, M. Hassan_Moradi, M. Tehrani-Doost, and V. Abootalebi, "Using non-linear features of EEG for adhd/normal participants' classification," *Procedia-Social and Behavioral Sciences*, vol. 32, pp. 148–152, 2012.

[11] S. Khoshnoud, M. A. Nazari, and M. Shamsi, "Functional brain dynamic analysis of adhd and control children using nonlinear dynamical features of EEG signals," *Journal of integrative neuroscience*, vol. 17, no. 1, pp. 17–30, 2018.

[12] M. Murias, J. M. Swanson, and R. Srinivasan, "Functional connectivity of frontal cortex in healthy and ADHD children reflected in EEG coherence," *Cerebral Cortex*, vol. 17, no. 8, pp. 1788–1799, 2007.

[13] M. Ahmadlou and H. Adeli, "Wavelet-synchronization methodology: a new approach for EEG-based diagnosis of ADHD," *Clinical EEG and neuroscience*, vol. 41, no. 1, pp. 1–10, 2010.

[14] A. Topic and M. Russo, "Emotion recognition based on EEG feature maps through deep learning network," *Engineering Science and Technology, an International Journal*, vol. 24, no. 6, pp. 1442–1454, 2021.

[15] O. K. Cura, A. Akan, G. C. Yilmaz, and H. S. Ture, "Detection of alzheimer's dementia by using signal decomposition and machine learning methods." *International Journal of Neural Systems*, pp. 2 250 042–2 250 042, 2022.

[16] Y. Li, J. Huang, H. Zhou, and N. Zhong, "Human emotion recognition with electroencephalographic multidimensional features by hybrid deep neural networks," *Applied Sciences*, vol. 7, no. 10, p. 1060, 2017.

[17] A. Benali Amjoud and M. Amrouch, "Convolutional neural networks backbones for object detection," in *International Conference on Image and Signal Processing*. Springer, 2020, pp. 282–289.